

$Q_A^{\cdot-}-Q_B$ state is destabilized by ~ 0.2 eV relative to $C-P_{Zn}^{++}-P-Q_A^{\cdot-}-Q_B$.

The lifetimes of the final charge-separated states in these pentad molecules are far longer than those observed for the simpler three- and four-part molecular devices that we have reported (1) but are substantially shorter than would be expected for direct charge recombination, on the basis of the results for related species. In this connection, it should be noted that in simpler triad systems, charge recombination occurs by a two-step reaction involving an intermediate species (8). A related mechanism may be operating here, although more studies will be necessary in order to elucidate the details of the process.

Although pentad 1 and related molecules differ significantly in structure from natural reaction centers, they do mimic several aspects of photosynthetic energy conversion. These include rapid singlet energy transfer to the primary donor, triplet energy transfer to the carotenoid, and a multistep electron transfer strategy that achieves efficient long-range and long-lived charge separation. There remain many important unanswered questions concerning natural photosynthesis that these artificial systems do not address or fail to mimic. However, pentad 1 does demonstrate that compounds can be designed in which electron transfer after photoexcitation occurs over several redox centers with a yield of near unity while conserving more than one-half of the excited-state energy of the primary donor. Thus, it appears that there is no a priori reason why the essential features of photosynthetic solar energy conversion cannot ultimately be reproduced successfully with man-made molecular devices (14).

REFERENCES AND NOTES

1. For a recent review, see D. Gust and T. A. Moore, *Science* **244**, 35 (1989).
2. The synthesis and characterization of this material will be reported elsewhere.
3. For a comprehensive review, see J. S. Connolly and J. R. Bolton, in *Photoinduced Electron Transfer*, Part D, M. A. Fox and M. Channon, Eds. (Elsevier, Amsterdam, 1988), chap. 6.2.
4. D. Gust *et al.*, *Photochem. Photobiol.*, in press.
5. J. Wandler and A. R. Holzwarth, *Biophys. J.* **52**, 717 (1987).
6. D. Gust *et al.*, *J. Am. Chem. Soc.* **110**, 321 (1988).
7. D. Gust *et al.*, *ibid.*, p. 7567.
8. D. Gust *et al.*, *ibid.* **108**, 8028 (1986).
9. F. S. Davis *et al.*, *Rev. Sci. Instrum.* **58**, 1629 (1987).
10. At 960 nm, the transient signal rises to $\sim 90\%$ of its maximum value with the response time of the instrument and reaches the peak value within several microseconds.
11. R. Bensasson, C. R. Goldschmidt, E. J. Land, T. G. Truscott, *Photochem. Photobiol.* **28**, 277 (1978). Quantum yields are based on published extinction coefficients for transient species (carotenoid radical cations and porphyrin triplet states), which are not accurately known (12). Excitation at 590 nm reduced the observed quantum yield to about 0.45. This wavelength-dependent quantum yield of charge separation is unusual; it does not occur in the

nonmetallated pentad and will be the subject of a future report (D. Gust *et al.*, in preparation).

12. T. A. Moore *et al.*, *Nature* **307**, 630 (1984).
13. J. A. Schmidt, A. Siemiarzuk, A. C. Weedon, J. R. Bolton, *J. Am. Chem. Soc.* **107**, 6112 (1985).
14. G. Ciamician, *Science* **36**, 385 (1912).
15. This work was supported by the Division of Chemical Sciences, Office of Basic Energy Sciences, Office of Energy Research, U.S. Department of Energy (DE-FG02-87ER13791) and the Department of

Energy University Research Instrumentation Program (DE-FG05-87ER75361). This is publication 43 from the Arizona State University Center for the Study of Early Events in Photosynthesis. The Center is funded by U.S. Department of Energy grant DE-FG02-88ER13969 as part of the U.S. Department of Agriculture-Department of Energy-National Science Foundation Plant Science Center Program.

10 October 1989; accepted 8 February 1990

Primary Sequence Information from Intact Proteins by Electrospray Ionization Tandem Mass Spectrometry

JOSEPH A. LOO, CHARLES G. EDMONDS, RICHARD D. SMITH*

Tandem mass spectrometry has been used to obtain information related to portions of the primary sequence for an intact protein, bovine ribonuclease A. Multiply charged molecular ions, generated by electrospray ionization, were collisionally dissociated at low energies in a triple quadrupole mass spectrometer to yield singly and multiply charged fragment ions that can be assigned to the known sequence of the protein. Dissociation of the highly charged molecular ions resulted in pairs of complementary product ions. The higher order (gas-phase) protein structure affects the dissociation processes, as observed in comparisons of tandem mass spectra of the native and disulfide-reduced forms of ribonuclease A.

MASS SPECTROMETRY (MS) AND tandem mass spectrometry (MS/MS) can be important tools in the determination of primary peptide and protein structure (1), especially for proteins that are blocked for conventional sequence analysis, that have undergone posttranslational modifications, or that are available only in small (picomole) quantities (2). However, facile MS analysis of larger polypeptides and proteins (molecular weights, M_r , greater than ~ 4000) will require the ability not only to form the gas-phase ions of the parent molecule, but also to cause the parent ion to undergo fragmentation processes so that sequence-related information can be obtained.

We report collision-induced dissociation (CID) tandem mass spectra for a multiply protonated intact protein, ribonuclease A (RNase A), produced by electrospray ionization (ESI), and demonstrate the feasibility of sequence-specific assignment of the product ion spectra. This analysis is accomplished, in part, by experimental methods that verify tentative CID product ion assignments based upon subsequent CID steps. Significant differences are found in MS/MS spectra of the native and reduced forms of RNase A, that is, after cleavage of disulfide bonds, suggesting that CID pro-

cesses are influenced by secondary or tertiary protein structure.

Although a number of competing methods exist for ionizing proteins, such as plasma desorption (PD) (3), laser desorption (4), and fast-atom bombardment (FAB) (5), ESI-MS shows potential as the method of choice for sensitive, rapid, and accurate molecular weight determination of large biomolecules (6-8) requiring as little as femtomole quantities (7). The atmospheric-pressure ESI source produces multiply charged (protonated) molecular ions from highly charged liquid droplets for proteins exceeding 100 kD; ions bearing more than 100 positive charges per molecule have been observed (7).

Tandem MS (9) has been used to determine primary structure for oligopeptides and, indirectly, proteins. The CID processes yield product ions characteristic of the amino acid sequence. More important, a range of possible modifications of oligopeptides can often be ascertained with speed and reliability (2, 10). Highly specific enzymatic digests of proteins followed by MS (FAB peptide mapping) and MS/MS of the peptide mixture can aid sequence determination of proteins (2, 10). Biemann (2) has discussed and demonstrated the enhanced speed of peptide and protein sequencing by such MS methods relative to conventional Edman degradation procedures (one residue per minute versus one residue per hour). High-performance liquid chromatography (HPLC) is often used to separate complex peptide mixtures to simplify the method

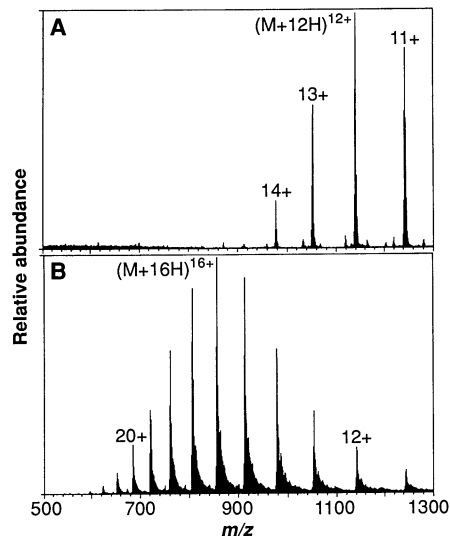
Chemical Methods and Separations Group, Chemical Sciences Department, Pacific Northwest Laboratory, Richland, WA 99352.

*To whom correspondence should be addressed.

Fig. 1. ESI mass spectra of (A) bovine pancreatic RNase A and (B) after reduction of its four disulfide bridges. The samples were dissolved in distilled water with 5% glacial acetic acid and delivered into the atmospheric-pressure ESI source at a flow rate of 0.5 $\mu\text{l}/\text{min}$. A liquid-sheath electrode of methanol is used (21), flowing at 2.5 $\mu\text{l}/\text{min}$, to establish electrical contact (+4 kV). Ions are sampled by a differentially pumped nozzle-skimmer interface adapted to a triple-quadrupole mass spectrometer (TAGA 6000E, Sciex, Thornhill, Ontario) having an m/z limit of 1400. Approximately 50 pmol of material was consumed to produce each spectrum.

prior to MS/MS analysis. However, little structural information for peptides and proteins with M_r greater than ~ 4000 has been obtained with FAB because of the reduced ion currents and the decrease in collisional activation efficiency as M_r increases (11). Tandem MS of the intact protein would further reduce the sequencing time by at least a factor equal to the number of peptide fragments generated from proteolytic digestion for subsequent MS/MS analysis.

Bovine pancreatic RNase A (M_r 13,682) is composed of 124 amino acid residues. Four disulfide bonds link Cys residues 26 to 84, 40 to 95, 58 to 110, and 65 to 72 (12). An extensive literature has been devoted to this molecule as a model for protein folding (13). The ESI mass spectra of RNase A and



its disulfide-reduced form (Fig. 1), which show a bell-shaped distribution of multiply charged $(M + nH)^{n+}$ ions (M represents the intact molecule and n the number of charges), are typical of ESI-MS of peptides and proteins (6–8). By assuming that adjacent peaks are separated by one charge state, any two peaks in an ESI mass spectrum of a pure compound allow for accurate determination of charge, and thus M_r (5–7). As previously reported (14), reduction of disul-

fide bonds allows the protein molecule to obtain a higher charge state by ESI, presumably by allowing for a more extended conformation. The $(M + 15H)^{15+}$ ion is the highest charged species observed for RNase A; however, upon reduction, the $(M + 23H)^{23+}$ species is detected.

Recently, we generated and used CID spectra from cytochrome *c* proteins ($M_r \sim 12$ kD) from a variety of species for identification (fingerprinting), but no sequence-related assignments were inferred (15). The interpretation of MS/MS spectra from large multiply charged parent ions is complicated by the size and complexity of the parent molecule, the diversity of potential product structures, and the large number of charge states for potential CID product ions (15–17). However, the use of MS/MS data from various parent charge states of the same molecule may alleviate the situation, if fragmentation behavior is similar. Furthermore, since dissociation of multiply charged parents may yield two (or more) product ions (as opposed to a singly charged precursor yielding only one singly charged product ion), complementary product-ion pairs that aid interpretation may often be present in the CID mass spectra. In the present study we observe simpler and more readily interpretable daughter ion spectra than in the

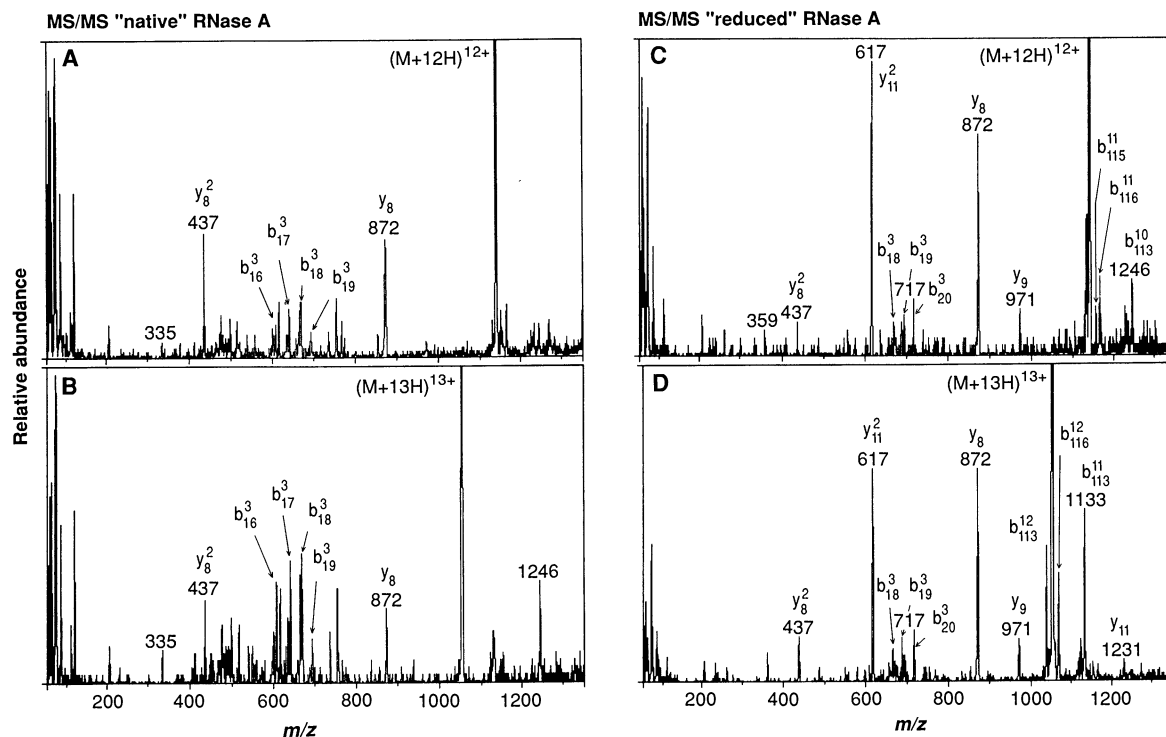


Fig. 2. MS/MS CID spectra from the (A) $(M + 12H)^{12+}$ and (B) $(M + 13H)^{13+}$ native species of RNase A and the (C) $(M + 12H)^{12+}$ and (D) $(M + 13H)^{13+}$ molecular ions from the reduced form. Parent ions selected by the first quadrupole (Q1) undergo CID through collisions with a neutral argon gas target ($8 \times 10^{13} \text{ cm}^{-2}$) in the second quadrupole (Q2). The resulting product ions are analyzed in the final quadrupole (Q3). Laboratory-frame collision energies were held constant at approximately

1820 eV. Conventional notation (2, 22) for sequence-specific fragmentation of polypeptides is used, augmented with a superscript indicating charge state (absence of a superscript indicates a singly charged ion). Briefly, the majority of fragment ions observed are due to cleavage of a CO–NH bond of the polypeptide backbone. The positive charge resides on the NH_2 -terminal fragment for b ions, whereas charge retention occurs at the COOH-terminal for y ions.

case of the cytochrome c proteins previously reported (15).

The CID product-ion mass spectra obtained with a tandem quadrupole mass spectrometer for the 12+ and 13+ charge states of native RNase A and the reduced form reveal higher relative intensities for product ions of the disulfide-reduced parent species (Fig. 2). For example, the ratio of the m/z (mass-to-charge ratio) 872 (y_8) ion to the parent ion intensity for both charge states of the reduced form shown in Fig. 2 is more than a factor of 2 greater than for the native protein. The y_8 ion, or its doubly charged version (y_8^2), is formed from the polypeptide backbone cleavage of the Val¹¹⁶ and Pro¹¹⁷ bond (with a single charge retained on the COOH-terminal portion). Other unusually intense peaks ascribed to cleavage of the NH₂-terminal amide bond of a Pro residue (Asn¹¹³ and Pro¹¹⁴ at m/z 617) are consistent with those observed for CID studies of smaller peptide molecules (17, 18). For the reduced state at constant laboratory-frame collision energies, the $[y_8]/[(M + nH)^{n+}]$ ratio gradually increases from 0.08 for $n = 12$ to 0.27 for $n = 17$.

Complementary ion pairs (which in sum account for the entire molecular ion) are a major feature of the reduced RNase A CID mass spectra. For example, with the $(M + 13H)^{13+}$ ion of reduced RNase A, the complement of the singly charged y_8 ion is the 12+ species, b_{116}^{12} . The y_{11} - b_{113}^{12} and y_{11}^2 - b_{113}^{11} pairs are also quite prominent. Spectra for other charge states studied (up to 17+) display peaks consistent with these assignments. Ions corresponding to y_8 , y_8^2 , and y_{11}^2 are present in the CID spectra with their complements, b_{116}^{n-1} , b_{116}^{n-2} , and b_{113}^{n-2} (where n is the parent-ion charge state), respectively. The region below m/z 400 contains small b and y type contributions due to dissociation occurring near both NH₂- and COOH-termini, in addition to immonium ions indicative of the presence of particular amino acid residues (18). A series of triply charged b_{14}^3 to b_{24}^3 ions (Asp¹⁴ to Asn²⁴) is observed between m/z 500 and 850 in the CID spectra of reduced RNase A, regardless of parent charge state.

Arguably, the more highly charged molecular ions incur a more extended (strained) conformation because of the mutual electrostatic repulsion of charge sites (7, 14). The presence of disulfide bridges restricts these extended conformations. A more extended (gas-phase) structure appears to substantially increase the rates of certain dissociation pathways. In contrast to smaller polypeptides, where such structural effects may be unlikely, the longer time required for energy equilibration and (perhaps much more importantly) conformational changes in larger

molecules may result in a much greater dependence upon gas-phase protein ion structure.

The atmosphere-vacuum interface of the ESI source can be used to add an additional fragmentation stage prior to the initial MS separation by CID between the voltage-biased nozzle and skimmer of the ion sampling region of the mass spectrometer. The CID products in such spectra (Fig. 3) arise from all charge states, but to different extents due to the dependence of collision energy upon charge state. Many peaks observed for the reduced species are also observed for the native form. For the reduced form (and presumably the more extended conformation), bond cleavage from the NH₂-terminal side (b_{21}^3 - b_{24}^3) occurs closer to the Cys²⁶ residue; COOH-terminal singly charged sequence ions, y_8 to y_{11} , are also observed in both forms of the protein along with some of the major complementary ions observed in the "conventional" CID spectra (Fig. 2).

Confirmation of tentative product-ion assignments can be obtained by CID in the second (radio frequency-only) quadrupole for CID product ions originally generated in the ESI atmosphere-vacuum interface. This extended CID/MS/CID/MS experiment [or MS/MS/MS (19)] is demonstrated for the peak at m/z 872, the prominent y_8 species occurring in all CID spectra of RNase A. Ions below m/z 872 are due to conventional sequence-specific fragmentation for the putative octapeptide (residues 117 to 124, Fig. 4). Additionally, no product ions were ob-

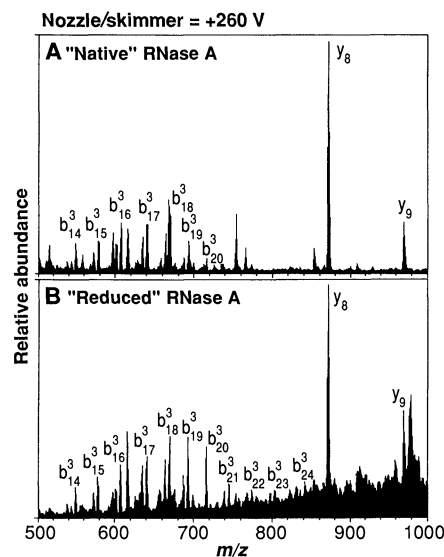


Fig. 3. ESI mass spectra of (A) native RNase A and (B) its disulfide-reduced state produced with an elevated nozzle/skimmer interface bias (+260 V). Sufficient collisional heating of the molecular ions has occurred to induce dissociation of most of the multiply charged molecular ions to form the sequence-specific ions labelled in the spectra.

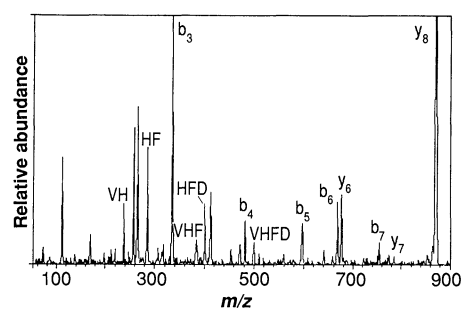


Fig. 4. CID mass spectrum of the m/z 872 fragment ion generated by CID in the atmosphere-vacuum sampling interface (nozzle/skimmer bias of +235 V). The resulting mass spectral pattern is consistent with the assignment of the m/z 872 ion as a y_8 singly charged species of RNase A, confirming the amino acid sequence of residues 117 to 124 (Pro-Val-His-Phe-Asp-Ala-Ser-Val). Fragmentation denoted with capital letters refer to "internal" sequence ions in which both NH₂- and COOH-terminal residues of the octapeptide have been lost (V, Val; H, His; F, Phe; and D, Asp).

served above m/z 872, consistent with the parent species being singly charged. Similar tandem mass spectra of other fragment parent ions shown in Fig. 3 can be obtained to confirm tentative CID assignments. Such experiments can directly probe regions of the molecule not accessible by CID of the intact molecule. In principle, Fourier transform mass spectrometry (FTMS) methods would facilitate an extended series of such steps (that is MS^m , where $m > 2$), providing a basis for more complete sequence assignments (20).

Sequence-specific fragmentation has been assignable for dissociation of an intact protein by mass spectrometry alone. The singly and multiply charged CID product ions were from regions primarily near the ends of the molecule. We note that our assignment of the RNase spectra was guided by previous knowledge of the protein sequence. In many cases, however, partial sequence information is available; examples include cases where only the gene sequence is available, or where homologous proteins are being examined. Although a relatively small fraction of the entire molecule is currently accessible by CID, alternative activation methods, such as photodissociation, or higher energy CID (as provided with sector instruments), may prove to be a more efficient fragmentation technique for generating sequence-related information. Ultrahigh m/z resolution, a unique capability of FTMS, would permit unambiguous product-ion charge-state determination (by observation of isotope peaks) and allow unknown sequences to be more easily interpretable and obtained. In combination with extended MS^m methods, obtaining complete sequence information for larger proteins may be feasible.

REFERENCES AND NOTES

1. C. J. McNeal, Ed., *The Analysis of Peptides and Proteins by Mass Spectrometry* (Wiley, Chichester, 1988).
2. K. Biemann and H. A. Scoble, *Science* **237**, 992 (1987); K. Biemann, *Biomed. Environ. Mass Spectrom.* **16**, 99 (1988).
3. B. Sundqvist *et al.*, *Science* **226**, 696 (1984); B. Sundqvist and R. D. Macfarlane, *Mass Spectrom. Rev.* **4**, 421 (1985); R. J. Cotter, *Anal. Chem.* **60**, 781A (1988).
4. M. Karas and F. Hillenkamp, *Anal. Chem.* **60**, 2299 (1988); M. Karas, U. Bahr, A. Ingendoh, F. Hillenkamp, *Angew. Chem.* **101**, 805 (1989).
5. M. Barber, R. S. Bordoli, G. J. Elliot, R. D. Sedgwick, A. N. Tyler, *Anal. Chem.* **54**, 645A (1982); M. Barber and B. N. Green, *Rapid Commun. Mass Spectrom.* **1**, 80 (1987).
6. C. K. Meng, M. Mann, J. B. Fenn, *Z. Phys. D* **10**, 361 (1988); M. Mann, C. K. Meng, J. B. Fenn, *Anal. Chem.* **61**, 1702 (1989); J. B. Fenn, M. Mann, C. K. Meng, S. F. Wong, C. M. Whitehouse, *Science* **246**, 64 (1989).
7. J. A. Loo, H. R. Udseth, R. D. Smith, *Anal. Biochem.* **179**, 404 (1989); C. G. Edmonds *et al.*, in *Proceedings of the Second International Symposium on Mass Spectrometry in the Health and Life Sciences*, A. L. Burlingame and J. A. McCloskey, Eds. (Elsevier, Amsterdam, in press).
8. T. R. Covey, R. F. Bonner, B. I. Shushan, J. Henion, *Rapid Commun. Mass Spectrom.* **2**, 249 (1988).
9. F. W. McLafferty, *Science* **214**, 280 (1981); F. W. McLafferty, Ed., *Tandem Mass Spectrometry* (Wiley, New York, 1983); K. L. Busch, G. L. Glish, S. A. McLuckey, *Mass Spectrometry/Mass Spectrometry: Techniques and Applications of Tandem Mass Spectrometry* (VCH, New York, 1988).
10. R. S. Johnson, W. R. Mathews, K. Biemann, S. Hopper, *J. Biol. Chem.* **263**, 9589 (1988); R. S. Johnson and K. Biemann, *Biochemistry* **26**, 1209 (1987); D. F. Hunt, J. R. Yates III, J. Shabanowitz, S. Winston, C. R. Hauer, *Proc. Natl. Acad. Sci. U.S.A.* **83**, 6233 (1986); E. J. Anderegge *et al.*, *Biochemistry* **27**, 4213 (1988).
11. M. L. Gross, K. B. Tomer, R. L. Cerny, D. E. Giblin, in *Mass Spectrometry in the Analysis of Large Molecules*, C. J. McNeal, Ed. (Wiley, Chichester, 1986), pp. 171-190; G. M. Neumann and P. J. Derrick, *Org. Mass Spectrom.* **19**, 165 (1984); G. M. Neumann, M. M. Sheil, P. J. Derrick, *Z. Naturforsch.* **39a**, 584 (1984).
12. D. G. Smyth, W. H. Stein, S. Moore, *J. Biol. Chem.* **238**, 227 (1963).
13. For example, see G. T. Montelione and H. A. Scheraga, *Acc. Chem. Res.* **22**, 70 (1989).
14. J. A. Loo, C. G. Edmonds, H. R. Udseth, R. D. Smith, *Anal. Chem.*, in press.
15. R. D. Smith, C. J. Barinaga, H. R. Udseth, *J. Phys. Chem.* **93**, 5019 (1989); R. D. Smith, J. A. Loo, C. J. Barinaga, C. G. Edmonds, H. R. Udseth, *J. Am. Soc. Mass Spectrom.* **1**, 53 (1990).
16. F. W. McLafferty, in *Mass Spectrometry in the Analysis of Large Molecules*, C. J. McNeal, Ed. (Wiley, Chichester, 1986), pp. 107-120.
17. C. J. Barinaga, C. G. Edmonds, H. R. Udseth, R. D. Smith, *Rapid Commun. Mass Spectrom.* **3**, 160 (1989).
18. S. A. Martin and K. Biemann, *Int. J. Mass Spectrom. Ion Processes* **78**, 213 (1987).
19. R. P. Grese, R. L. Cerny, M. L. Gross, *J. Am. Chem. Soc.* **111**, 2835 (1989).
20. M. V. Buchanan, Ed., *Fourier Transform Mass Spectrometry: Evolution, Innovation, and Application* (American Chemical Society, Washington, DC, 1987).
21. R. D. Smith, C. J. Barinaga, H. R. Udseth, *Anal. Chem.* **60**, 1948 (1988).
22. P. Roepstorff and J. Fohlman, *Biomed. Mass Spectrom.* **11**, 601 (1984).
23. We thank H. A. Scheraga and F. W. McLafferty (Cornell University) for the RNase A samples, and acknowledge the U.S. Department of Energy, through internal Exploratory Research of the Molecular Research Center under contract DE-AC06-76RLO 1830, the National Science Foundation Instrumentation and Instrument Development Program (DIR 8908096), and the NIH Office of Human Genome Research (GM 42940), for support of this research. Pacific Northwest Laboratory is operated by Battelle Memorial Institute.

16 November 1989; accepted 14 February 1990

Holocene Mean Uplift Rates Across an Active Plate-Collision Boundary in Taiwan

CHUNG-HO WANG AND WILLIAM C. BURNETT

Samples of Holocene fossil coral from uplifted reefs of three tectonically distinct, yet geographically proximal regions of Taiwan have been dated by uranium-series and ¹⁴C isotopes. Applying corrections for altitude change caused by sea level fluctuations enables evaluation of long-term average Holocene uplift rates for three areas across an active convergent margin: (i) the Hengchun Peninsula of the Eurasian tectonic plate; (ii) the Eastern Coastal Range of Taiwan, a plate boundary; and (iii) two offshore islands, Lanyu and Lutaο, both situated on the leading edge of the adjoining Philippine Plate. The data indicate that while all three areas have experienced uplift through the Holocene, plate collision has caused significantly higher uplift rates in the region directly along the plate boundary.

TECTONICALLY, TAIWAN IS OF GREAT interest because a major plate boundary, separating the Eurasian and Philippine tectonic plates, runs through its eastern section. Geophysical studies have shown that eastern Taiwan is seismically and geodetically active as a result of ongoing collision (1, 2). To some degree, collision also seems to be taking place to the west, as the Eurasian Plate is subducted and the accretionary wedge is pushed by the Philippine Plate. Geodetic surveys and tidal observations spanning several years have shown that the modern uplift rate of eastern Taiwan is as high as 35 mm/year, among the

highest known in the world (3). Although uplift rates are known to be high, few studies have attempted to assess how these rates vary across a convergent margin, and whether uplift is temporally constant or intermittent. To address these questions, we examined long-term (thousands of years) uplift rates on both sides of the Taiwan collision boundary, as well as in the boundary zone itself.

The distribution of raised coral reef terraces in Taiwan is such that we were able to evaluate uplift rates for different parts of the collisional boundary by collecting samples from three locations (Fig. 1): (i) the Eastern Coastal Range (the northern extension of the Luzon Arc and in the boundary zone between the Eurasian and Philippine tectonic plates), (ii) the Hengchun Peninsula (on the main island of Taiwan, lying directly on

the accretionary wedge overlying the Eurasian Plate), and (iii) two islands off the southeastern coast of Taiwan, Lanyu and Lutaο (both on the Philippine plate). Our sample set allowed us to evaluate relative uplift from three close, yet tectonically distinctive settings, that is, the leading edges of two large tectonic plates and their zone of active collision.

In an earlier study, Peng *et al.* (4) summarized 34 radiocarbon ages of uplifted Holocene corals sampled at elevations up to 25 m above present sea level from the Hengchun Peninsula and Eastern Coastal Range of Taiwan. That study showed that average long-term uplift rates are 5.3 mm/year for southern Taiwan and 5.0 mm/year for the Eastern Coastal area. Our additional data and sampling points allow a more complete assessment of the long-term geodetic changes along the plate boundary as well as in those areas more removed from the collision zone during the Holocene.

Because fossil corals are suitable for both uranium-series and ¹⁴C dating, and are known to grow within a limited depth range, they are ideal samples for neotectonic studies. Coral segments, mostly of the *Favidae* and *Poritidae* species, were trimmed to remove the outer, somewhat weathered crust and were ultrasonically cleaned to ensure that no terrestrial contaminating materials remained (5). All samples were analyzed by x-ray diffraction, and only those containing less than approximately 2% calcite, a recrystallized product of the original aragonite, were used for isotopic analysis (6). The height of each sample was deter-

C.-H. Wang, Institute of Earth Sciences, Academia Sinica, Post Office Box 23-59, Taipei, Taiwan, Republic of China.

W. C. Burnett, Department of Oceanography, Florida State University, Tallahassee, FL 32306.